A model for transport and agglomeration of particles in reactive ion etching plasma reactors

Fred Y. Huang,[a] Helen H. Hwang,[b] and Mark J. Kushner[c]
Department of Electrical and Computer Engineering, University of Illinois, Urbana, Illinois 61801

(Received 4 October 1995; accepted 11 December 1995)

Dust particle contamination of wafers in reactive ion etching (RIE) plasma tools is a continuing concern in the microelectronics industry. It is common to find that particles collected on surfaces or downstream of the etch chamber are agglomerates of smaller monodisperse spherical particles. These observations, and the fact that the forces which govern the transport and trapping of particles are partly determined by their size, place importance on understanding particle growth and agglomeration mechanisms. Since individual particles in plasma etching tools are negatively charged, their agglomeration is problematic since the particles must obtain sufficient kinetic energy to overcome their mutual electrostatic repulsion. In this article, we discuss results from a model for particle agglomeration in RIE plasma tools with which we address the transport of particles and interparticle collisions resulting in agglomeration. These results indicate that the rate and extent of particle agglomeration depend on the particle density, plasma power deposition, and, to a lesser degree, gas flow. The dependence of agglomeration on rf power results from the fact that the kinetic energy of a dust particle is largely determined by its acceleration by ion drag forces. Significant agglomeration may occur in particle traps where the particle density is large.

I. INTRODUCTION

Dust particle contamination is a continuing concern in plasma processing discharges used for semiconductor device manufacturing.[1] These discharges are typically low gas pressure (tens to hundreds of mTorr and operate with electron densities of 10^9–10^{11} cm^{-3}. The typical sizes of contaminating particles are hundreds of nm to a few microns. With the advent of submicron feature sizes in microelectronic devices, dust contamination by even the smaller particles may result in a killer defect. Therefore, controlling the generation and transport of particles in plasma processing discharges is of great interest to the semiconductor manufacturing community.

The mechanics of transport and trapping of particles in low pressure etching and deposition plasma tools has been studied by several authors.[2–5] Briefly, the trajectories of dust particles are governed by a variety of mechanical and electrical forces, the latter resulting from the fact that dust particles typically charge negatively in plasmas. These forces include ion drag, electrostatic, neutral drag, thermophoretic, gravitational, and self-diffusion. Ion drag forces accelerate particles in the direction of the net ion flux, typically towards the boundaries of the reactor. Electrostatic forces accelerate the negatively charged particles towards the maximum in the plasma potential, typically in the center of the plasma. Fluid drag results from entrainment of the dust particles in the bulk gas flow in the reactor. The characteristic trapping of dust particles often observed at the sheath edges[1] results from an equilibrium between the ion drag and electrostatic forces, an equilibrium that can be disrupted by a sufficiently high gas flow.

It is a common observation that particles collected on surfaces in reactive ion etching (RIE) tools or downstream of the plasma chamber are actually clusters of agglomerates of smaller, monodisperse spherical particles.[6–8] (For purposes of discussion, we will refer to these smaller, monodisperse particles as ''primary'' particles.) The implication of these observations is that primary particles grow to a terminal size, and then agglomerate to form larger structures. The agglomeration is problematic since the dust particles are usually electrically charged negative, which requires that the reactants in an agglomerating collision have sufficient kinetic energy to overcome the mutual electrostatic repulsion. For example, the agglomeration of two 1 μm radius Si dust particles having 5000 elementary charges each requires center-of-mass speeds of >1 m s^{-1}.

In this article, we discuss results from a computational study of agglomeration of particles using a newly developed model for dust particle agglomeration in RIE plasma tools. The particle agglomeration model (PAM) addresses the transport of dust particles under the influence of all cited forces, as well as collisions between particles. The purpose of this study is to identify the operating conditions (power, flow rate, particle sizes) that lead to particle agglomeration. We found that particle agglomeration preferentially occurs at higher discharge powers and with larger primary particles. The former trend results from the larger kinetic energy imparted to the particles by ion drag, thereby allowing the particles to overcome their electrostatic repulsion. The latter trend results from the manner in which electrostatic and ion drag forces scale with particle size (ion drag forces dominate for larger particles). We also find that particle agglomeration

[a]Electronic mail: f-huang@uiuc.edu
[b]Electronic mail: h-hwang@uiuc.edu
[c]Electronic mail: mjk@uiuc.edu

proceeds more rapidly for high aspect ratio particles that are rodlike (as opposed to spherical particles).

II. DESCRIPTION OF THE MODEL

We have previously described a dust particle transport model (DPTM) with which we simulated the trajectories of dust particles under the influence of electrostatic, ion drag, gravitational, thermophoretic, and fluid-drag forces.[3] The PAM uses the DPTM as a point of departure. The DPTM will be briefly described, followed by a discussion of the additional algorithms in the PAM.

The DPTM integrates the trajectories of computational pseudoparticles under the influence of the cited forces. The DPTM obtains the ion fluxes, electric fields, and neutral flow field required to calculate these forces from a companion model called the hybrid plasma equipment model (HPEM). The HPEM is described in detail in Ref. 9. Briefly, it is a modular two-dimensional simulation of plasma etching or deposition equipment in which continuity and momentum equations are solved for all charged and neutral species, and Poisson's equation is solved for the electric potential. Electron impact source functions and transport coefficients are provided by an electron Monte Carlo simulation. The DPTM has been revised from that described in Ref. 3 by incorporating the same numerical meshes and material identification schemes used in the HPEM. The DPTM now also uses the expressions for the ion drag cross sections derived by Kilgore *et al.*[10] as opposed to directly calculating those quantities by using the particle-in-cell simulation described in Ref. 11.

The PAM uses the same algorithms and methodology to calculate the forces on particles and advance their trajectories as in the DPTM. Particle–particle interactions are additionally included on a particle-mesh basis using Monte Carlo algorithms. The PAM begins by distributing pseudoparticles representing dust particles with a preselected spatial distribution. The equations of motion of the pseudoparticles are then advanced. The spatial locations of the pseudoparticles are periodically ''binned'' onto the numerical mesh to provide a dust particle density at each spatial point. These densities are then used to compute collision frequencies between all pseudoparticles in a given computational cell. The collision frequencies are based on the overlap of the particles' Debye–Huckel shielding volumes. To determine the occurrence of a particle–particle collision, we use Monte Carlo techniques based on the time interval between binnings and the calculated particle collision frequencies. A given pseudoparticle collides with one of the other pseudoparticles in the spatial cell if

$$\Delta t \geqslant -\frac{\ln(r)}{\nu_D}, \tag{1}$$

where Δt is the time between binning, $r=(0,1)$ is a randomly distributed number, and ν_D is the particle collision frequency based on the overlap of Debye–Huckel shielding volumes.

In the event of a ''shielding volume collision,'' one of the particles in the numerical cell is chosen as the collision partner. The collision partner is that particle which satisfies

$$\frac{\nu'_{j-1}}{\nu_D} \leqslant r \leqslant \frac{\nu'_j}{\nu_D}, \quad \nu'_j = \sum_{i=1,\,j} \nu_j, \tag{2}$$

where r is another random number (0,1) and ν'_j is the cumulative collision frequency for the jth particle in the cell. Given the two particles which are now collision partners, their velocities and masses are used to calculate the center-of-mass kinetic energy of the pair, ϵ. Given that the maximum repulsive electrostatic potential between the particles is

$$U = \frac{1}{4\pi\epsilon_0}\frac{Q_1 Q_2}{d}, \tag{3}$$

where Q_1 and Q_2 are the charges on the two particles, and d is their distance of closest approach, an agglomeration collision can occur if $\epsilon \geqslant U$. If this is the case, a random impact parameter is selected to determine the occurrence of a physical collision. If a physical collision does occur, the particles agglomerate, conserving total volume, mass, and momentum. Otherwise, they maintain their current velocity and trajectory or are deflected by the electrostatic repulsive forces.

The shape of the agglomerates may prove important in understanding their growth. Currently, the PAM allows for two particle shapes, spherical and cylindrical. The shape of the particle enters into the calculation of the charge on the particle given its electrical potential, V. The electrical potential of the particle is based on balancing electron and ion fluxes to its surface.[3] The effective charge Q on a particle is given by $Q=CV$, where C is the particle's capacitance. For a spherically shaped particle of radius R, the capacitance is

$$C = 4\pi\epsilon_0 R\left(1+\frac{R}{\lambda_D}\right), \tag{4}$$

where λ_D is the linearized Debye length.[5] For a finite cylindrical particle with length L and radius R, the capacitance is approximately

$$C = \frac{2\pi\epsilon_0 L}{\ln(\lambda_D/R)} + \frac{2\pi R^2\epsilon_0}{\lambda_D}, \tag{5}$$

where the second term approximates the contribution from the two ends of the particle.

The distance of closest approach between two spherical particles in the PAM is the sum of their radii. Cylindrical particles can, however, impinge at random orientations resulting in different distances of closest approach. To account for this effect, when two cylindrical particles (or a spherical and cylindrical particle) collide, we randomly choose the distance of closest approach and orientation based on the radius and length of each of the colliding particles. The shape of the agglomerated particle depends on the orientation and shape of the colliding particles. If we force all particles and agglomerates to be spheres, the newly formed agglomerate is simply a larger sphere whose dimensions are determined by conserving mass. Otherwise, for example, if two cylindrical particles collide ''head to tail,'' the resulting agglomerate is

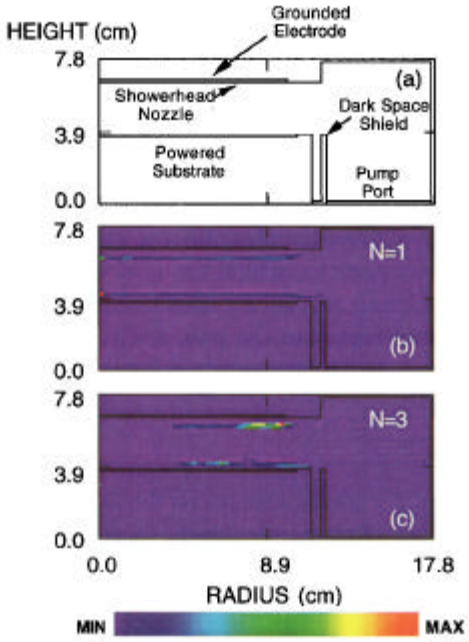

FIG. 1. Time integrated trajectories of (b) primary particle and (c) timer agglomerates in a RIE plasma tool (Ar, 100 mTorr, 12 W). A schematic of the reactor is shown in (a). The primary particles are 1.5 μm in radius and the agglomerate is spherical. Agglomeration at low power typically occurs in and near trapping sites.

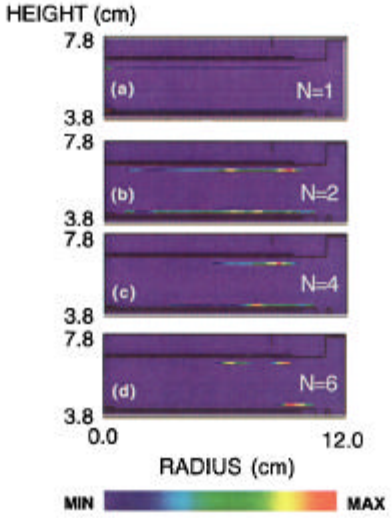

FIG. 2. Time integrated trajectories of spherical agglomerates for the conditions of Fig. 1 except that the rf power is 120 W. (a) Primary particles, (b) second order, (c) fourth order, and (d) sixth order agglomerates. The larger kinetic energies of the particles produced by ion drag at the higher rf power allows higher order agglomerates to form at locations more distributed through the reactor.

also a cylinder, but of smaller aspect ratio (aspect ratio is defined as $\Gamma = R/L$). The precise L and R of the agglomerate are chosen based on the overlap length of the colliding cylindrical particles in such a manner as to conserve mass. In doing so, we can form long, thin cylindrical particles ($\Gamma \ll 1$) or flat disks ($\Gamma \gg 1$).

III. AGGLOMERATION OF PARTICLES IN RIE PLASMA TOOLS

A schematic of the RIE reactor we used in this study is shown in Fig. 1(a). The lower electrode is powered at 13.56 MHz and is surrounded by a grounded dark space shield. The upper electrode is grounded and contains a showerhead nozzle. The annular pump port is at the bottom of the reactor. The electrodes' diameters are 20 cm and their separation is 2.8 cm. The gas is Ar at 100 mTorr. The dusty densities used in the simulations are 10^2–10^4 cm^{-3}, which is sufficiently small so that the electron energy distributions and plasma potentials are not significantly affected.[12] The maximum plasma density for an applied rf voltage amplitude of 75 V (48 W) is 3×10^{10} cm^{-3}. The simulation time for all cases discussed here is 0.5 s which is sufficient for steady state conditions to be obtained. Time integrated "fluence" contours of dust particle trajectories are shown in Figs. 1(b) and 1(c) for a primary particle 1.5 μm in radius and for spherical agglomerates having up to three primary particles. The power deposition is 12 W and there is no gas flow. Primary particles are trapped in two thin layers near the sheath edge of the top and bottom electrodes. Agglomerates having three primary particles are generated only in regions of high primary particle density, which in this geometry are trapping locations near the edge of the wafer. Here the collision frequencies between primary particles are large enough to generate the higher order cluster. These agglomerates represent only a small fraction (less than a few percent) of the total dust particle population. The low rate of agglomeration results from the low acceleration of dust particles by ion drag. The low acceleration results in smaller kinetic energies which are unable to overcome the mutual electrostatic repulsion of the particles.

Fluence contours of the dust particle trajectories for a rf power of 120 W are shown in Fig. 2 for spherical agglomerates having up to six primary particles. As the power increases, agglomerates both grow to larger sizes (that is, contain more primary particles) and constitute a larger fraction of the total dust density. With increasing rf power, ion drag forces are proportionally larger, thereby accelerating particles to higher speeds. Second order agglomerates are more abundant and take on a spatial distribution similar to the primary particle population. The agglomerates represent a substantially larger portion of the dust particle inventory (several percent). With the additional kinetic energy provided by the larger ion drag forces, dust particles both collide more frequently and have more energy to overcome the repulsive potential barriers of their collision partners and agglomerate. Since agglomerating particles must have a large *relative* speed, one finds agglomeration typically occurring between fast primary particle entering a trapping site and nearly stationary particles already at the trapping site. Therefore, at moderate rf powers (tens of W), large agglomerates are typically only found near true trapping sites, while at higher powers (>100 W), large agglomerates can be generated in quasitraps above the entire substrate surface.

The size of the primary dust particle plays an important

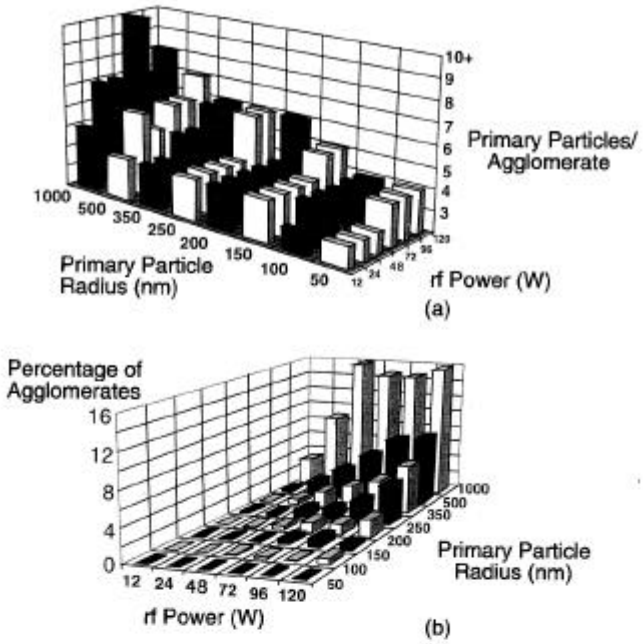

FIG. 3. Agglomerate properties as a function of primary particle size and rf power. (a) Maximum agglomerate size and (b) relative agglomerate population. The degree of agglomeration increases with both power and size of the primary particle due to the inability of the particles to more effectively overcome electrostatic barriers. In addition, the amount of agglomeration increases as well, resulting in a higher agglomerate-to-primary particle ratio.

role in particle trapping. Larger dust particles are typically trapped closer to surfaces in RIE reactors since they are more sensitive to ion drag forces. There is a similar dependence for agglomeration. The maximum number of primary particles/agglomerate observed over a range of rf powers and primary particle sizes is shown in Fig. 3(a). In general, higher power and larger primary particle sizes produce higher degrees of agglomeration. This scaling with primary particle size results from the fact that the repulsive forces scale as $Q^2R \sim C^2/R \sim R$, whereas the kinetic energy of the particles scales as $MV^2 \sim R^3V^2$. The increased sensitivity to ion drag of larger particles compensates for their lower rates of acceleration due to their larger mass, which allows favorable scaling for larger particles to overcome electrostatic repulsion. The end result is agglomeration which favors larger primary particles and higher rf powers, provided that the powers are not so large that ion drag forces push small agglomerates through the sheaths. The fraction of the total particle population that is agglomerates is shown in Fig. 3(b). In addition to growing larger at higher powers and primary particle sizes, the relative amount of agglomeration increases as well.

Agglomeration does result from particle–particle interactions, and therefore the rates of agglomeration are sensitive to the total primary particle inventory. The relative densities of agglomerates are shown in Fig. 4 as a function of average primary particle density for a rf power of 48 W. Both the number of agglomerates formed and the extent of agglomeration increase with increasing primary particle density.

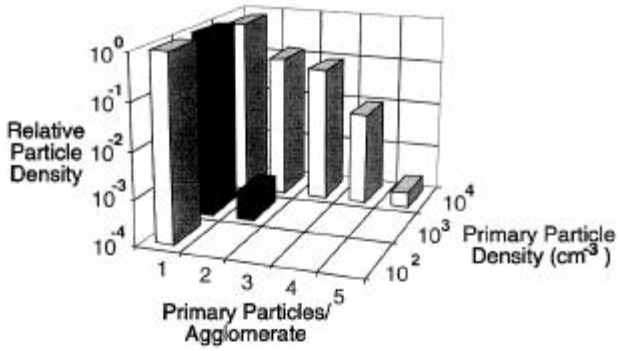

FIG. 4. Relative densities of agglomerates as a function of primary particle density (rf power=48 W, primary particle size=0.2 μm). Increasing primary particle densities increases the collision frequency, thereby producing higher degrees of agglomeration.

Clearly, for a given power deposition and reactor geometry, which determine the particle trapping locations, there is a density threshold below which no agglomeration occurs.

Large gas flows from a showerhead or laterally across the wafer in a RIE reactor have proven to be very useful in controlling contamination of the substrate. For example, simulations using our DPTM model have shown that gas flows of hundreds of sccm can sweep trapped dust particulates away from the substrate and electrodes. We investigated the effect of gas flow using the PAM model and found similar scaling for agglomeration. For example, fluence contours are shown in Fig. 5 for 1 μm primary particles and five primary particle agglomerates at a rf power of 72 W with gas flow (225 sccm) and without gas flow. Without gas flow, primary particles trap and agglomerates form over the substrate and electrode surfaces. With gas flow, primary particles are swept to the outer regions of the reactor, and agglomerates form predominantly outside of the electrode gap. The additional kinetic energy imparted to the particles by fluid drag may also contribute to agglomeration.

The shape of the agglomerates in part defines their rates of agglomeration for at least two reasons. First, the capaci-

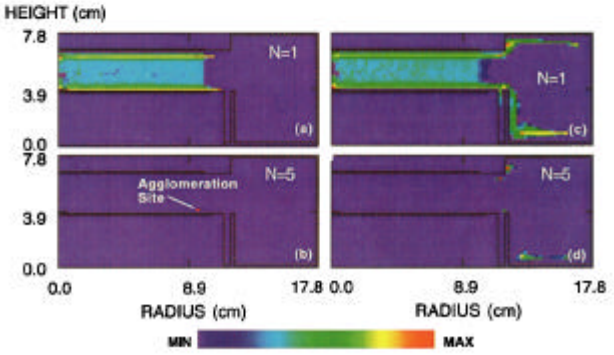

FIG. 5. Time integrated trajectories of primary particles and fifth order agglomerates. (a), and (b): Without gas flow; (c), (d): with a gas flow of 225 sccm. The neutral gas flow sweeps primary particles away from the substrate resulting in agglomeration outside the electrode gap.

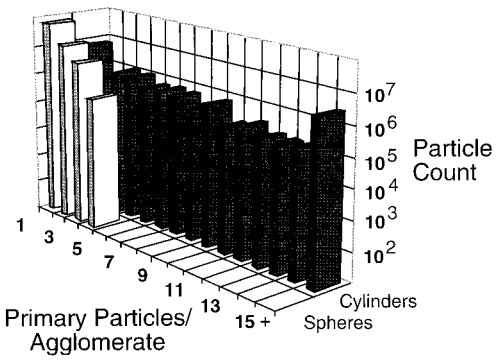

FIG. 6. Relative densities of agglomerates (rf power=120 W) for spherically and cylindrically shaped particles. The primary particle size is 0.2 μm. Cylindrically shaped particles result in a higher degree of agglomeration.

tance (and hence charge) of the agglomerate depends on the shape of the particle. Second, the orientation (and distance of closest approach) of colliding particles also depends on their respective shapes. Both of these dependencies can be illustrated by the agglomeration of a spherical primary particle with a long string of already agglomerated spherical primary particles. For a sufficiently long string (length $>\lambda_D$), the approaching primary particle electrostatically ''sees'' only the charge on one end of the string, thereby reducing the repulsive forces. The charge on the long string is also remote from the approaching particle. This effect is much less severe for spherical agglomerates. To illustrate this scaling, we parameterized the PAM for otherwise identical conditions while specifying that the agglomerates be only spherical or allowing them to take on cylindrical shapes. The resulting particle counts are shown in Fig. 6 for a power deposition of 120 W and primary particle sizes of 0.2 μm. Cylindrical particles agglomerate to a greater degree for at least two reasons. First, the cylindrical particles, on average, have a larger distance of separation between the charge centers. Second, the cylindrical particles have a smaller capacitance and thus a lower amount of charge on them. The combination of these two effects creates a lower average electrostatic potential to overcome between colliding particles, and results in a significantly higher degree of agglomeration for the cylindrical particles. Agglomerates in excess of 15 primary particles are generated.

IV. CONCLUDING REMARKS

We have developed a particle agglomeration model (PAM) to investigate the formation of large particles in RIE plasma tools. Agglomeration between particles is modeled using particle mesh and Monte Carlo techniques. In order to agglomerate, dust particles must have sufficient kinetic energy to overcome the electrostatic potential barrier between them. Results from the PAM indicate that these conditions are met at high rf powers and large primary particle sizes. Under conditions of homogeneous nucleation, smaller particles usually undergo more agglomeration since agglomeration scales as the square of the particle density and typically there are more smaller particles. To some degree, that is true here as well. However, under conditions where there is a lower limit to the size of the primary particle, as is the case when primary particles are monodisperse in RIE discharges, the larger the primary particle, the more rapid the rate of agglomeration. The shape of the particle influences the rate of agglomeration. Typically, nonspherical particles having narrow aspect ratios agglomerate at a higher rate and to larger sizes.

ACKNOWLEDGMENTS

This work was supported by the Semiconductor Research Corporation, Sandia National Laboratories/Sematech, the National Science Foundation (Grant Nos. ECS94-04133 and TS94-12565), and the University of Wisconsin Engineering Research Center for Plasma Aided Manufacturing.

[1]G. S. Selwyn, Plasma Sources Sci. Technol. **3**, 340 (1994).
[2]A collection of articles addressing particle transport in plasma processing reactors appears in a special issue of Plasma Sources Sci. Technol. **3**, August (1994).
[3]S. J. Choi, P. L. G. Ventzek, R. J. Hoekstra, and M. J. Kushner, Plasma Sources Sci. Technol. **3**, 418 (1994).
[4]D. J. Rader and A. S. Geller, Plasma Sources Sci. Technol. **3**, 426 (1994).
[5]D. B. Graves, J. E. Daugherty, M. D. Kilgore, and R. K. Porteous, Plasma Sources Sci. Technol. **3**, 433 (1994).
[6]P. D. Haaland, A. Garscadden, B. Ganguly, S. Ibrani, and J. Williams, Plasma Sources Sci. Technol. **3**, 381 (1994).
[7]W. J. Yoo and Ch. Steinbrüchel, J. Vac. Sci. Technol. A **10**, 1041 (1993).
[8]R. N. Carlile, J. F. O'Hanlon, L. M. Hong, M. P. Garrity, and S. M. Collins, Plasma Sources Sci. Technol. **3**, 334 (1994).
[9]P. L. G. Ventzek, R. J. Hoekstra, and M. J. Kushner, J. Vac. Sci. Technol. B **12**, 461 (1994).
[10]M. D. Kilgore, J. E. Daugherty, R. K. Porteous, and D. B. Graves, J. Appl. Phys. **73**, 7195 (1993).
[11]S. J. Choi and M. J. Kushner, IEEE Trans. Plasma Sci. **22**, 138 (1994).
[12]M. J. McCaughey and M. J. Kushner, Appl. Phys. Lett. **55**, 951 (1989).